

TANAKA *ET AL.* reply—First, we would like to correct the term “mantle array” in the summary of ref. 1 to crustal array. We originally used the term crustal array to distinguish the clear $\epsilon_{\text{Ce}}-\epsilon_{\text{Nd}}$ array, but the term was changed in the editing of our manuscript. It was pointed out in ref. 1 that continental crustal rocks form a clearly defined ‘crustal array’, whereas mantle-derived rocks are dispersed on a $\epsilon_{\text{Ce}}-\epsilon_{\text{Nd}}$ diagram. Dickin claimed that the $\epsilon_{\text{Ce}}-\epsilon_{\text{Nd}}$ array of mantle-derived rocks (mantle array) should be sharp, as defined in Fig. 1, and that three basalts examined in ref. 1 should exist within his mantle array. We demonstrate here that (1) Ce isotopes of these basalts are not abnormal, judging from the geochemical behaviour of REE; and (2) mantle mixing is not the omnipotent to confine the isotopic values within his narrow mantle array.

The ϵ_{Ce} and ϵ_{Nd} variation in the mantle must be a result of many geochemical factors, namely La/Ce and Sm/Nd (parent/daughter) ratios, integration time of daughter nuclides, and mixing effect. Quantitative estimation of the extent of the latter two cases is difficult. Reliable rare earth element (REE) data for mantle material are few, because of alteration. Generally Mid-Ocean Ridge Basalt (MORB) is considered to have a REE pattern similar to that of mantle. Chond-

rite-normalized La/Ce-Sm/Nd diagrams for MORB and ocean island basalt (OIB) (exclude IAB) is shown in Fig. 2a. They plot with a negative correlation passing the second, third and fourth quadrants. Although MORB reflects the mantle REE pattern, partial melting and fractionation processes modify the REE pattern to be light REE (particularly La) rich. Then, the source mantle of MORB is expected to have a slightly smaller La/Ce ratio than MORB (left side in the data distribution area in Fig. 2a). S_1-S_2 in Fig. 2a are the points of model REE patterns S_1-S_3 in Fig. 2 of ref. 1. They plot just along a possible mantle La/Ce-Sm/Nd trend. S_2 and S_3 clearly represent the possible MORB source as stated in ref. 1. Mantle variation trend S_1-S_4 does not meet the origin. This is the reason why $\epsilon_{\text{Ce}}-\epsilon_{\text{Nd}}$ variation of S_1-S_4 has fan-like shape (see Fig. 3 of ref. 1). Dickin argues that a sharp mantle array stands on a mantle mixing model. Although a basic gneiss (sample 8X) in ref. 3 is not a mantle material, the 8X is a La-depleted material derived directly from a chondritic source³. Its La-depleted REE pattern (Fig. 1 of ref. 3) may be acceptable as one of the analogues of an isolated domain of depleted mantle. We examined a homogenization of isolated depleted mantle (8X) with undepleted (chondritic) mantle

and plotted the 8X sample on the top of Fig. 1b. The mixing curve definitely passes through the right-hand outside of Dickin's mantle array region.

The crustal rocks have various REE patterns with convex and concave shapes as well as a log-linear shape in their La-Sm span. Then it is natural that $\epsilon_{\text{Ce}}-\epsilon_{\text{Nd}}$ data are plotted on both sides of the $\epsilon_{\text{Ce}} = -0.112\epsilon_{\text{Nd}}$ line. Some Amitsoq gneisses are also slightly apart from the line (Shimizu *et al.*, unpublished). Chondrite-normalized La/Ce-Sm/Nd values of rocks forming continental crust (most of the rocks are from Precambrian terrane) are examined in Fig. 2b. Generally, they plot in the fourth quadrant of the diagram with negative correlation. L_1-L_3 and data for samples 16-19 of ref. 1 plot along the axial part in the whole distribution. Then, $\epsilon_{\text{Ce}} = -0.112\epsilon_{\text{Nd}}$ is considered to be an axis of the $\epsilon_{\text{Ce}}-\epsilon_{\text{Nd}}$ plot.

Interference and base line checks in our isotope measurements are already presented in refs 1 and 4. Possible interferences and peak tailing are always monitored during the measurements. On the quality of the data, we would like to emphasize that all of the data sets in ref. 1 are obtained from single solution, which provides a coherent data set among Ce and Nd isotopes and REE abundances, especially for crystalline acidic rocks.

Dickin prefers a rather smaller decay constant to $2.58 \times 10^{-12} \text{ yr}^{-1}$ on the basis of his geologic determination³. His data with trondhjemite 16Y show a rather large deviation. The trondhjemite bodies are generally intrusive to other gneiss types (ref. 5) and the REE pattern of sample 16Y is quite different from others (see Fig. 1 of ref. 3). Trondhjemite also has not been used for Sm-Nd age determination⁶. It should be excluded from La-Ce age determination. Recalculation excluding trondhjemite 16Y gives far better deviation (means square weighted deviates = 1.18). In this case, a bigger decay constant $\lambda_{\text{La}} = 2.68 \times 10^{-12} \text{ yr}^{-1}$ gives a coherent La-Ce age ($2,900 \pm 390 \text{ Myr}$ (2σ)) with Sm-Nd age ($2,910 \text{ Myr}$).

T. TANAKA

Geological Survey of Japan,
Higashi 1-1-3,
Tsukuba 305,
Japan.

H. SHIMIZU
Y. KAWATA
A. MASUDA

Department of Chemistry,
University of Tokyo,
Hongo, Tokyo 113,
Japan

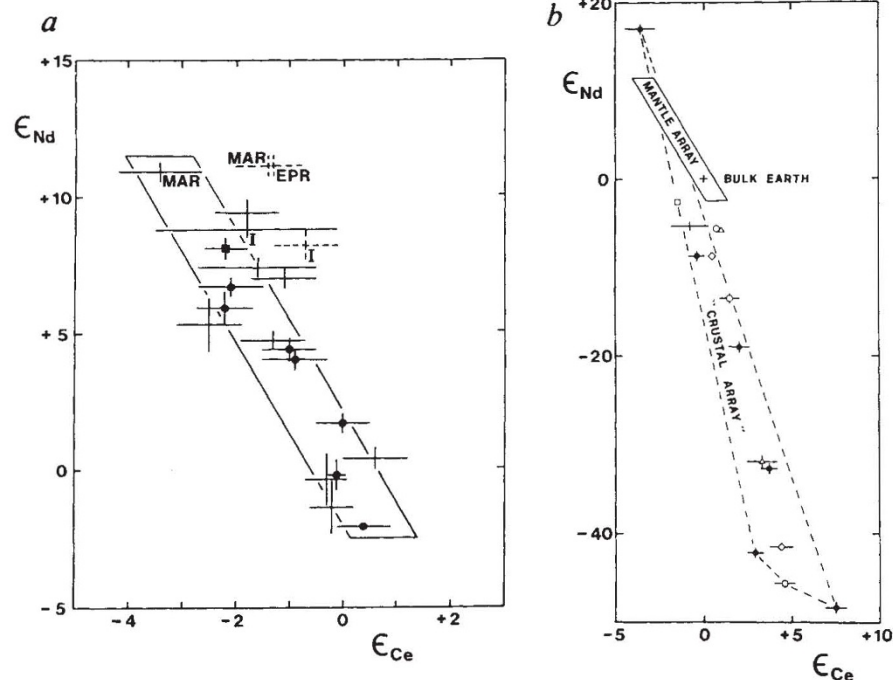


Fig. 2 $\log(\text{La}/\text{Ce})_S/(\text{La}/\text{Ce})_{\text{CH}}$ versus $\log(\text{Sm}/\text{Nd})_S/(\text{Sm}/\text{Nd})_{\text{CH}}$ diagrams for MORB and OIB (a), and for metamorphic and sedimentary rocks forming continental crust (b). Suffixes S and CH indicate rock sample and chondrite. $(\text{La}/\text{Ce})_{\text{CH}} = 0.377$ and $(\text{Sm}/\text{Nd})_{\text{CH}} = 0.325$ are used. These values correspond to $^{138}\text{La}/^{142}\text{Ce} = 0.00306$ and $^{147}\text{Sm}/^{144}\text{Nd} = 0.1966$. Large solid circles and small solid circles show the data obtained by isotope dilution mass spectrometry (IDMS) and by other techniques respectively. Several data are lying outside the area. Chondrite-normalized $\log(\text{Sm}/\text{Nd})_S/(\text{Sm}/\text{Nd})_{\text{CH}}$ values smaller than -0.35 are the data for extremely differentiated minor rock unit. Open circles S_1-S_3 and L_1-L_3 correspond to the REE pattern of S_1-S_3 and L_1-L_3 in Fig. 2 of ref. 1, respectively. Solid diamonds show data for samples 16-19 of ref. 1. List of refs used for data points are available from the authors on request.

1. Tanaka, T., Shimizu, H., Kawata, Y. & Masuda, A. *Nature* **327**, 113-117 (1987).
2. Dickin, A.P. *Nature* **326**, 283-284 (1987).
3. Dickin, A.P. *Nature* **325**, 337-338 (1987).
4. Tanaka, T. & Masuda, A. *Nature* **300**, 515-518 (1982).
5. Weaver, B.L. & Tarney, J. *Earth planet. Sci. Lett.* **51**, 279-296 (1980).
6. Hamilton, P.J., Evensen, N.M., O'Nions, R.K. & Tarney, J. *Nature*, **277**, 25-28 (1979).